Numerical characterization of the dynamics of vortex filaments in round jets

M. Abid and M. E. Brachet
Laboratoire de Physique Statisque, CNRS URA 1306, ENS Ulm, 24 Rue Lhomond, 75231 Paris Cedex 05, France

(Received 5 March 1993; accepted 13 July 1993)

The dynamics of streamwise vorticity in axisymmetric jets is studied by direct numerical integration of the Navier–Stokes equations coupled with a passive scalar. Consistently with recent experiments and inviscid numerical simulations, the present viscous simulations show the appearance of pairs of axially counter-rotating vortex filaments. After their formation the filaments move away from the jet, dragging the tracer into finger-shaped structures. The three-dimensional topology of the rings, filaments, and fingers is described, well beyond the time of filament formation. Finally, visualizations of the pressure gradient field are presented, which suggest that the filaments can be directly observed experimentally by seeding the flow with microbubbles.

The dynamics of spreading, entrainment, and mixing in constant-density axisymmetric jets occurs primarily via finger (or mushroom)-shaped structures.[1,2] These structures have also been observed in hot jets and uniform density acoustically forced jets.[3,4] They are known in this context as "side jets." In the case of hot jets, a self-oscillating "preferred" mode for the jet,[5] and the acoustic forcing in the second case, lead to the formation of high-intensity vortex rings. Strong vortex rings, produced by the fastest growing Kelvin–Helmholtz mode, are also present in constant-density unforced jets.[1,2]

Based on experimental results[2,4] and inviscid numerical simulations[6,7] the generation of side jets has been related to the expulsion of fluid by pairs of counter-rotating longitudinal vortex filaments. These filaments are, in turn, produced[7] by a mechanism analogous to the one generating axial vortices in mixing layers (see, e.g., Ref. 8 [Fig. 21(a,b)], p. 238, for the equivalent of side jets in mixing layers) via condensation of the vorticity ribbons connecting the primary vortices.[9–11] Martin and Meiburg,[7] using inviscid vortex method computations, have characterized the initial spontaneous formation of counter-rotating streamwise filaments and related them to the experimental visualizations of lobe structures.[6] However, inviscid calculations do not allow the study of flow dynamics beyond the time of longitudinal filament formation, as they have to be terminated at that time because of loss of resolution, due to the absence of viscosity.

In this Letter, we use direct simulation of the three-dimensional incompressible Navier–Stokes equations to characterize the dynamics of axisymmetric jets. We also solve the equation of a passive scalar:

$$\partial_t \rho + (\mathbf{u}\cdot\nabla)\rho = \nu\Delta\rho. \tag{1}$$

This passive scalar, which has no effect on the velocity field, is used only as a numerical tracer to visualize the mixing between the interior and exterior of the jet.

To integrate the Navier–Stokes equations and (1) numerically, we use a standard pseudospectral method.[12] The flow is taken to be periodic along the axis of the jet, and is expanded in sine or cosine functions in the lateral directions. Although they do not take into account the spatial spreading of the flow, note that such temporal calculations are known, in the case of mixing layers, to capture the essential features of the vorticity dynamics.[8] The use of Fourier transforms adapted to this geometry reduces the computation time and storage by a factor of 4 relative to a general periodic code. Time stepping is carried out by a second-order-accurate Adams–Bashforth/Crank–Nicholson scheme. The code uses multitasking, and one time step at a resolution of $32\times80\times80$ takes 2 CPU seconds on a CRAY 2 computer.

The initial condition is a superposition of the basic profile of the jet and several unstable eigenmodes from linear stability theory. The basic profile is that studied by Michalke:[13]

$$u(r) = (U_0/2)\{1+\tanh[(R-r)/2\theta]\}, \tag{2}$$

where U_0 is the centerline speed, θ is the momentum thickness, r is the distance to the axis, and R is the radius of the jet. The unstable modes are obtained by solving the Rayleigh equation by a shooting method and interpolating the solutions onto the grid points of the pseudospectral code. The passive scalar is initialized with the same profile as (2).

We checked the three-dimensional code by reproducing the growth rates predicted by linear theory for sufficiently small amplitudes of the unstable mode. We then followed the nonlinear temporal evolution of the dynamics of the jet. The calculations presented here were carried out for a relative thickness $\theta/R=0.08$, at Reynolds number $\mathrm{Re}=U_0\theta/\nu=200$ and used a resolution of $64\times160\times160$.

The initial amplitude of the most linearly unstable mode was chosen so that saturation would occur approximately at $tU_0/R=3.5$ At this time, the tracer distribution in a plane containing the jet's axis shows a characteristic roll up due to the saturation of the Kelvin–Helmholtz instability into vortex rings (data not shown).

Further evolution of the jet occurs via instability to nonaxisymmetric perturbations. This evolution therefore

 0899-8213/93/5(11)/2582/3/$6.00

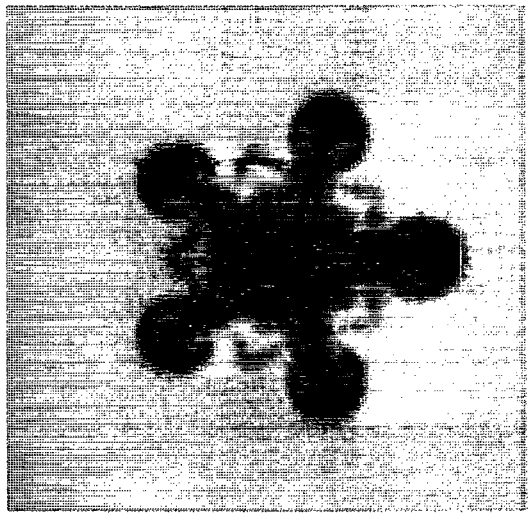

(a)

(b)

FIG. 1. Visualization of the density of the passive scalar in a plane perpendicular to the axis of the jet at $tU_0/R=10.24$. Secondary perturbation with wave number $m=\pm 5$. (a) is a cut between vortex rings and (b) is a cut near a vortex ring. Note that the ejection of the tracer leads to the formation of fingerlike structures.

depends on the nonaxisymmetric perturbations present in the initial condition. In the case of a perturbation with azimuthal wave number $m=\pm 5$, Fig. 1 shows visualizations of the tracer in cross sections perpendicular to the axis of the jet. Figure 1(a) is a cross section midway between vortex rings, and Fig. 1(b) near a vortex ring. Both ejections of the tracer in fingerlike structures and concentrations toward the interior of the jet are visible. We have obtained similar results for initial perturbations with $m=\pm 3$, $m=\pm 4$, or $m=\pm 6$ with, respectively, 3, 4, and 6 fingers (data not shown). Figure 2 shows the same visualization when the nonaxisymmetric initial perturbation is an isotropic random Gaussian noise, with spectrum cutoff at scales smaller than $\theta/2$. While finger shaped structures are also present in this case note the appearance of spiral roll-up of the tracer. The numerical visualizations presented in Figs. 1 and 2 are in good qualitative agreement with the experimental visualizations of Yule,[1] Monkewitz,[3,4] and Liepmann and Gharib[2] for different stations in the jet.

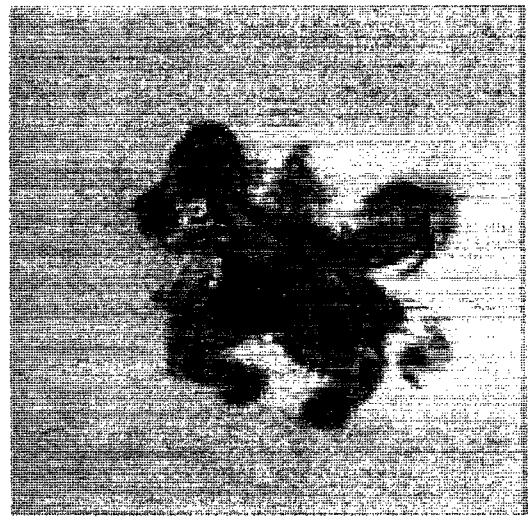

FIG. 2. Same as Fig. 1(a) but with random nonaxisymmetric secondary perturbation. Note the presence of both fingerlike structures and spiral structures.

The origin of the side jets can be understood by looking at Fig. 3, a three-dimensional visualizations of the vorticity field $\omega=\nabla\times\mathbf{u}$ and of the gradient of the tracer. Figure 3 shows that the initial perturbation with azimuthal wave number $m=\pm 5$ evolves spontaneously into five pairs of counter-rotating filaments located between the vortex rings formed by the Kelvin–Helmholtz instability. The rings themselves display a waviness characteristic of Widnall's

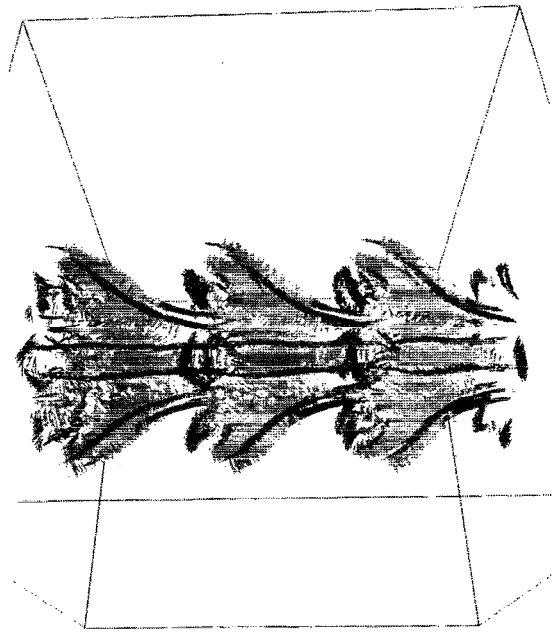

FIG. 3. Visualization of the vorticity field (dark) and of the gradient of the passive scalar (grey) (same conditions as in Fig. 1). Note that the passive scalar gradients are located between the vortex filaments.

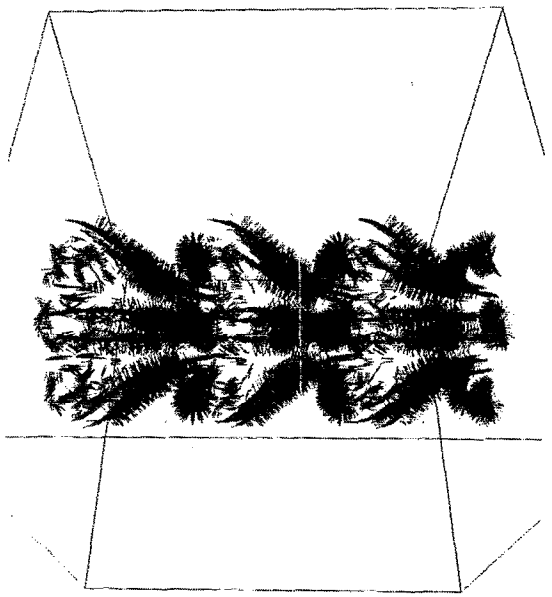

FIG. 4. Visualization of the pressure gradient (grey) and vorticity (dark). Same conditions as in Fig. 3. Note the presence of strong pressure gradients around the filaments.

instability.[14] Note that the disconnected appearance of the rings is due to the threshold applied by the graphics software used to visualize the vector field: only the 4000 largest vectors are shown.

The gradient of the tracer is seen in Fig. 3 to be localized between the rings, showing that the basic mechanism for the generation of side jets is the dragging of fluid by the counter-rotating axial filament pairs that migrate away from the central jet. Each axial filament originates outside a vortex ring and terminates inside the following ring along the jet. Detailed examination of the three-dimensional visualizations shows that the filaments double their number of partners as they enter a vortex ring. Here, we witness the tracer being drawn into the jet. Similar visualizations (data not shown) in the case of the random perturbation show that the spiral structures are generated by isolated (i.e., unpaired) vortex filaments.

Finally, Fig. 4 show the pressure gradient field (in grey). The presence of strong pressure gradients near the vortex filaments suggests that they can be observed experimentally by seeding the flow with microbubbles. Pressure-induced forces will make the bubbles migrate toward the filaments where they will concentrate. This experimental method, that has already been used to study turbulence,[15] would shed new light on the dynamics of vortex filaments in transitional round jets.

ACKNOWLEDGMENTS

Our computations were carried out on the CRAY 2 of the Centre de Calcul Vectoriel pour la Recherche. The three-dimensional visualizations were performed using the VFFS software package developed at CERFACS.

This research was supported by DRET Contract No. 90-173.

[1] A. J. Yule, "Large-scale structure in the mixing layer of a round jet," J. Fluid Mech. **89**, 413 (1978).
[2] D. Liepmann and M. Gharib, "The role of streamwise vorticity in the near-field entrainment of round jets," J. Fluid Mech. **245**, 643 (1992).
[3] P. A. Monkewitz, B. Lehmann, B. Barsikow, and D. W. Bechert, "The spreading of self-excited hot jets by side jets," Phys. Fluids A **1**, 446 (1989).
[4] A. Monkewitz and E. Pfizenmaier, "Mixing by 'side jets' in strongly forced and self-excited round jets," Phys. Fluids A **3**, 1356 (1991).
[5] C. M. Ho and P. Huerre, "Perturbed free shear layers," Annu. Rev. Fluid Mech. **16**, 365 (1984).
[6] E. Meiburg, J. C. Lasheras, and J. E. Martin, "Experimental and numerical analysis of the three-dimensional evolution of an axisymmetric jet," in *Turbulent Shear Flows* (Springer-Verlag, Berlin, 1991), Vol. 7, p. 195.
[7] J. E. Martin and E. Meiburg, "Numerical investigation of three-dimensionally evolving jets subject to axisymmetric and azimuthal perturbations," J. Fluid Mech. **230**, 271 (1991).
[8] R. W. Metcalfe, S. A. Orszag, M. E. Brachet, S. Menon, and J. J. Riley, "Secondary instability of a temporally growing mixing layer," J. Fluid Mech. **184**, 207 (1987).
[9] S. J. Lin and J. M. Corcos, "The effect of plane strain on the dynamics of streamwise vortices," J. Fluid Mech. **141**, 139 (1984).
[10] J. C. Neu, "The dynamics of a columnar vortex in an imposed strain," Phys. Fluids **27**, 2397 (1984).
[11] J. C. Neu, "The dynamics of stretched vortices," J. Fluid Mech. **143**, 253 (1984).
[12] D. Gottlieb and S. A. Orszag, *Numerical Analysis of Spectral Methods: Theory and Applications* (SIAM, Philadelphia, PA, 1977).
[13] A. Michalke, "Survey on jet instability theory," Prog. Aeroesp. Sci. **21**, 159 (1984).
[14] S. E. Widnall, D. B. Bliss, and C. Y. Tsai, "The instability of short waves on a vortex ring," J. Fluid Mech. **66**, 35 (1974).
[15] S. Douady, Y. Couder, and M. E. Brachet, "Direct observation of the intermittency of intense vorticity filaments in turbulence," Phys. Rev. Lett. **67**, 983 (1991).